

Synthesis and Electrochemistry of the Monolacunary Dawson-Type Tungstoarsenate $[\text{H}_4\text{AsW}_{17}\text{O}_{61}]^{11-}$ and Some First-Row Transition-Metal Ion Derivatives

Israel-Martyr Mbomekalle,^[a] Bineta Keita,^[a] Yu Wei Lu,^[a] Louis Nadjio,^{*,[a]}
Roland Contant,^[b] Nebebech Belai,^[c] and Michael T. Pope^[c]

Keywords: Polyoxometalates / Dawson dissymmetrical polyoxometalates / Arsenic / Tungsten / Electrochemistry / Electrocatalysis

The novel family of the Dawson-type tungstomonoarsenate $[\text{H}_4\text{AsW}_{18}\text{O}_{62}]^{7-}$ has been extended by preparing for the first time its monolacunary species and its first-row transition-metal ion substituted derivatives. All compounds were characterized by elemental analysis, IR and UV/Vis spectroscopy and representative examples by ^{183}W NMR spectroscopy. Several lines of experimental evidence converge to indicate that the substitution occurs in the α_2 position. The lacunary species, unlike its phosphorus analogue, was sufficiently stable for a few voltammetric runs. Therefore, the cyclic vol-

tammetric properties of substituted compounds were studied as a function of pH and systematically compared with those of the lacunary precursor rather than with those of their analogues derived from the symmetrical species $[\text{As}_2\text{W}_{18}\text{O}_{62}]^{6-}$. The electrocatalytic properties of all compounds were illustrated by the reduction of nitrite by reduced $[\text{H}_4\text{AsW}_{18}\text{O}_{62}]^{7-}$ and of nitrate by reduced $\alpha_2\text{-}[(\text{H}_2\text{O})\text{Cu}(\text{H}_4\text{AsW}_{17}\text{O}_{61})]^{9-}$.

(© Wiley-VCH Verlag GmbH & Co. KGaA, 69451 Weinheim, Germany, 2004)

Introduction

Polyoxometalates (POMs) are early transition metal–oxygen anionic clusters. They simultaneously exhibit many properties that make them attractive for applications in catalysis, separations, imaging, materials science and medicine.^[1–8] The scope for varying the atomic compositions of these complexes is virtually enormous and new structures continue to be discovered. Even though complete rationalisation of the construction of these structures is lacking at present, very many of them might be recognised as being derived, at least partly, from lacunary Keggin and Dawson fragments. Recently, we have been interested in the possibility of obtaining Dawson structures with two different central heteroatoms. We were stimulated by the pioneering work^[9] of one of the present authors who reported the synthesis of the novel Dawson-type tungstophosphate

$[\text{H}_4\text{PW}_{18}\text{O}_{62}]^{7-}$ and its lacunary and zinc-substituted derivatives $[\text{H}_4\text{PW}_{17}\text{O}_{61}]^{11-}$ and $[\text{Zn}(\text{H}_2\text{O})(\text{H}_4\text{PW}_{17}\text{O}_{61})]^{9-}$. In these species, the two anionic halves are of the A-type with only one of them containing a central heteroatom in the +v oxidation state. Soon afterwards, our group confirmed the feasibility of this synthesis for the As^V-containing analogue,^[10] also obtaining the corresponding trilacunary species and achieving the synthesis of two sandwich-type derivatives, $[\text{Zn}_4(\text{H}_2\text{O})_2(\text{H}_4\text{AsW}_{15}\text{O}_{56})_2]^{18-}$ and $[\text{Cu}_4(\text{H}_2\text{O})_2(\text{H}_4\text{AsW}_{15}\text{O}_{56})_2]^{18-}$. With a systematic study of the relevant parameters, we have also established^[11] the best experimental conditions for the synthesis of $[\text{H}_4\text{AsW}_{18}\text{O}_{62}]^{7-}$ and demonstrated that these conditions are essentially different from those necessary to obtain the well-known symmetric species $[\text{As}_2\text{W}_{18}\text{O}_{62}]^{6-}$. The same kind of rationalisation was achieved in the comparable syntheses of $[\text{P}_2\text{W}_{18}\text{O}_{62}]^{6-}$ and $[\text{H}_4\text{PW}_{18}\text{O}_{62}]^{7-}$.^[12,13] Recently, we have extended the work on this new family of dissymmetric Dawson-type heteropolyanions to the first-row transition-metal ion substituted derivatives of $[\text{H}_4\text{PW}_{18}\text{O}_{62}]^{7-}$.^[13]

Herein, we report the synthesis, characterization and electrochemistry of the hitherto unknown monolacunary species of $[\text{H}_4\text{AsW}_{18}\text{O}_{62}]^{7-}$ and its first-row transition-metal ion substituted derivatives. Their electrochemistry reveals differences from the corresponding symmetric heteropolyanions and with the phosphorus analogues. In addition, an evaluation of their electrocatalytic properties for the reduction of nitrate and nitrite is provided.

^[a] Laboratoire de Chimie Physique, UMR 8000, CNRS, Electrochimie et Photoélectrochimie, Université Paris-Sud, Bâtiment 420, 91405 Orsay Cedex, France
Fax: (internat.) + 33-1-69154328
E-mail: nadjo@lcp.u-psud.fr

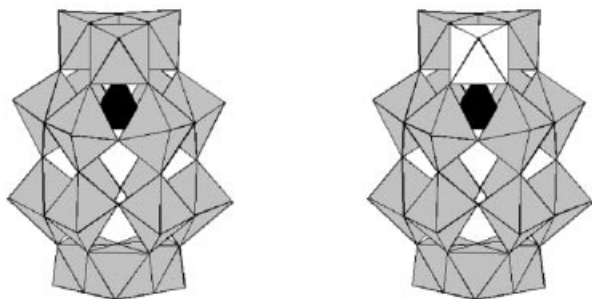
^[b] Laboratoire de Chimie Inorganique et des Matériaux Moléculaires, UMR 7071, CNRS, Université Paris VI, 4, place Jussieu, 75252 Paris Cedex 05, France

^[c] Department of Chemistry, Georgetown University, Box 571227, Washington, DC 20057, USA

Supporting information for this article is available on the WWW under <http://www.eurjic.org> or from the author.

Results and Discussion

Prolonged heating of the reaction mixture during the synthesis of $[\text{H}_4\text{AsW}_{18}\text{O}_{62}]^{7-}$ results in the formation of the pure so-called α -isomer.^[11] All the POMs in the present study are primarily derived from α - $[\text{H}_4\text{AsW}_{18}\text{O}_{62}]^{7-}$ (AsW_{18}) and their formulae will be written as MasW_{17} , with omission of oxygen atoms and overall charges when no confusion is likely to arise; M represents the substituent metal cation. In close analogy with the case of α - $[\text{H}_4\text{PW}_{18}\text{O}_{62}]^{7-}$, the results of electrochemistry and IR spectroscopy demonstrate that the mild alkaline degradation of AsW_{18} results in the removal of a W atom from the “cap” in the half of this molecule containing the single As atom, thus creating the first vacancy in one of the so-called α_2 positions. Scheme 1 illustrates the α -structure proposed for α - $[\text{H}_4\text{AsW}_{18}\text{O}_{62}]^{7-}$ and one of its monosubstituted derivatives, α_2 - $[\text{M}(\text{H}_2\text{O})\text{H}_4\text{AsW}_{17}\text{O}_{61}]^{9-}$, where M represents a divalent transition metal ion and the water molecule is omitted.



Scheme 1. Schematic representations of the Dawson-type tungstomonoarsenate and a monosubstituted tungstomonoarsenate

Synthesis

The synthesis and purification of $[\text{H}_4\text{AsW}_{18}\text{O}_{62}]^{7-}$ has been described previously in detail.^[11] As will be described in the Exp. Sect., the monolacunary derivative was obtained under mild conditions, provided the addition of KHCO_3 was sufficient to maintain the pH around 8 during the process. Two slightly different experimental conditions were applied for the synthesis of metal cation substituted derivatives, depending on the terminal ligand on the substituent metal atom in the final product. As is usual with Keggin- and Dawson-type POMs, the sixth coordination site on the metal atom in the 1:1 complexes may be occupied by a variety of ligands.^[1,13] We were interested in two kinds of ligands: on one hand, in the substitution by $\text{V}^{5+/4+}$ or $\text{Mo}^{6+/5+}$, the terminal oxo group can be considered to reconstitute the structure of a saturated POM; on the other hand, for all other metal cations of interest in this work, the sixth position is occupied by a water molecule.

UV/Vis and IR Spectroscopic Characterisation

As expected, no specific fingerprint signals were found in the UV/Vis spectra in the series in order to distinguish one compound from the next. However, recording these spectra

over a period of at least 24 h was helpful in assessing the stability of the complexes as a function of pH. This delay was selected as a compromise between the time needed for electrochemical characterisation of the complexes and that for eventual long-lasting or preparative-scale catalytic or electrocatalytic processes. The precursor lacunary $\text{H}_4\text{AsW}_{17}$ was found to be sufficiently stable for a few cyclic voltammetric runs to be performed, a remarkable difference from its phosphorus analogue for which no stability domain could be found. The so-called “saturated” substituted compounds, MasW_{17} (M = Mo or V), show stabilities close to that of the unsubstituted compound, with complete stability observed from pH = 0.3 to 4. Table 1 shows complementary details as well as the stability domains for all the other substituted derivatives. Black indicates the domain in which a particular derivative is stable; dark grey corresponds to a decomposition less than or equal to 20% and light grey indicates a decomposition of between 20 and 70%. It is worth pointing out the complete identity of this behaviour with that of the corresponding phosphorus analogues, except for the difference in stability of their respective monolacunary derivatives.^[12] The only exception concerns the Cu derivatives. CuAsW_{17} is stable from pH = 0.3 to 5 and CuPW_{17} is only stable from pH = 2 to 5.

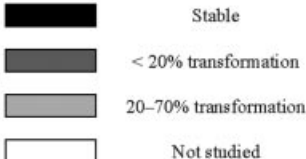
The locations of the main IR bands are summarized in the Supporting Information and show a comparison between As_2W_{18} and AsW_{18} (Table SII). Substitution into the vacancy of the lacunary species AsW_{17} can be expected to restore the symmetry present in AsW_{18} , at least as far as IR spectra are concerned. Then, only a relative weakening of the bond force constants would be mainly expected as a result of substitution. Table SII confirms this general trend, even though the observed variations are modest. Despite this, the IR spectra support the conclusion that no important structural changes appear from one compound to the next.

^{183}W NMR Spectroscopy

Table 2 shows the ^{183}W NMR chemical shifts for the Zn- and Ni-monosubstituted derivatives of the Dawson-type tungstomonophosphate and tungstomonoarsenate. The chemical shifts for the corresponding tungstodiphosphates were obtained from the pioneering work of Jorris and co-workers^[14] and are shown for comparison. The chemical shifts measured in this work compare well with those of the corresponding MP_2W_{17} . In full agreement with expectations, all tungsten centres can be observed for the Zn-substituted anions, as shown in the Supporting Information (Figure SII). Peak integrations confirm this observation (Table 2). The signals of all tungsten atoms, except two pairs, are seen for the Ni-substituted anions. It is likely that the two lines observed at low field are from the two remaining belt tungsten atoms in the XW_9 half of the anion. The Fe- and Cu-substituted derivatives were too paramagnetic to give useful results.

Table 1. Stability, monitored by UV/Vis spectroscopy as a function of pH over 24 h for α -As₂W₁₈, α -AsW₁₈ and the α_2 -AsW₁₇M derivatives of the latter complex

pH	0.3	1	2	3	4	5	6	7	8
α -As ₂ W ₁₈									
α -AsW ₁₈									
α_2 -AsW ₁₇ Mo									
α_2 -AsW ₁₇ V ^(IV)									
α_2 -AsW ₁₇ V ^(V)									20–40%
α_2 -AsW ₁₇ Mn									
α_2 -AsW ₁₇ Fe									
α_2 -AsW ₁₇ Co									
α_2 -AsW ₁₇ Ni									
α_2 -AsW ₁₇ Cu									
α_2 -AsW ₁₇ Zn									



Stable
 < 20% transformation
 20–70% transformation
 Not studied

Table 2. Comparison of ¹⁸³W NMR chemical shifts of MXW₁₇ where M = Zn or Ni and X = As or P with transition-metal monosubstituted Wells-Dawson heteropolytungstates from ref.^[14]

Compound	¹⁸³ W NMR chemical shifts	Ref.
α_2 -[(D ₂ O)Zn ²⁺ P ₂ W ₁₇ O ₆₁] ⁸⁻	–84.4 (2 W), –138.7 (2 W), –180 (1 W), –186.7 (2 W), –208.6 (2 W), –214.8 (6 W), –242.7 (2 W)	[14]
α_1 -[(D ₂ O)Zn ²⁺ P ₂ W ₁₇ O ₆₁] ⁸⁻	–99.4, –117.4, –123.0, –146.1, –151.9, –157.7, –167.6, –174.2, –175.7, –177.3, –193.3, –200.1, –203.7, –210.3, –214.1, –214.6, –225.5 (each 1 W)	[14]
[Zn(H ₄ PW ₁₇ O ₆₁)] ⁹⁻	–98 (2 W), –135 (2 W), –147 (2 W), –176 (2 W), –195 (2 W), –200 (2 W), –205 (2 W), –208 (2 W), –222 (1 W)	this work
[Zn(H ₄ AsW ₁₇ O ₆₁)] ⁹⁻	–85 (2 W), –137 (2 W), –166 (2 W), –169 (2 W), –175 (2 W), –191 (4 W), –201 (2 W), –228 (1 W)	this work
α_2 -[(D ₂ O)Ni ²⁺ P ₂ W ₁₇ O ₆₁] ⁸⁻	+468.3 (2 W), +338.7 (2 W), –142 and –146 (4 W), –200 and –202 (3 W), –230.5 (2 W)	[14]
[Ni(H ₄ PW ₁₇ O ₆₁)] ⁹⁻	+468 (2 W), +386 (2 W), –140 (2 W), –164 (2 W), –167 (2 W), –187 (2 W), –245 (1 W)	this work
[Ni(H ₄ AsW ₁₇ O ₆₁)] ⁹⁻	+613 (2 W), +349 (2 W), –140 (2 W), –153 (2 W), –160 (2 W), –175 (2 W), –246 (1 W)	this work

A comparison of the results in Table 2 strongly suggests that the substitution site is the α_2 position, in complete analogy with the phosphorus systems.^[12]

Electrochemistry

We have previously shown by cyclic voltammetry, the difference in basicity between the several first reduction species of As₂W₁₈ and AsW₁₈.^[10] Typically, in a pH = 0.3 sulfate medium, the part of the pattern of As₂W₁₈ of interest here consists of two one-electron waves followed by two two-electron waves. These waves correspond to reversible diffusion-controlled processes. In contrast, in the same medium, AsW₁₈ exhibits three two-electron chemically reversible diffusion-controlled waves. As a cross-check, the first wave was also shown by controlled potential coulometry to feature a two-electron process. Furthermore, we found that this first wave split into two one-electron waves at pH = 4 while the pattern for As₂W₁₈ did not change. This behaviour can be understood in terms of the higher basicity of the first several reduced species of AsW₁₈ over those of As₂W₁₈. The complete analogy between this and the comparable behaviour of PW₁₈ and P₂W₁₈ must be stressed.^[12]

The electrochemistry of monosubstituted derivatives of AsW₁₈ can be discussed straightforwardly in comparison with the corresponding As₂W₁₈-derived analogues. Owing to the marginal variations in the behaviour of the corresponding compounds from one series to the next, the main outcome of such a study turned out to be the confirmation that α_2 -substituted derivatives were indeed formed in the MAsW₁₇ series.

In contrast to the lacunary species PW₁₇, its analogue AsW₁₇ is sufficiently stable to allow a few voltammetric runs in the pH = 3 and pH = 5 media used. This observation opens up the way for comparison between the electrochemical behaviour of MAsW₁₇ derivatives with that of their precursor lacunary compound. Such a comparison is appropriate because those substituted derivatives bearing a terminal water molecule as the sixth ligand on the substituent metal cation are expected to behave much like the lacunary precursor, at least as far as the electrochemistry of the POM framework is concerned.^[15–18] In addition, the differences brought about by the presence of As instead of P in MXW₁₇ (X = P or As) were selected as a basis for further interesting comparisons. In short, two issues were

found pertinent for this electrochemical study: (i) the redox behaviour of the electroactive substituent cations within the POM framework and (ii) the influence of the nature of the substituent cation and of the central heteroatom on the reduction of the W^{VI} centre.

Redox Behaviour of the Electroactive Substituent Transition Metal Ions within MAsW_{17}

The reduction or oxidation peak potentials for reducible or oxidizable cations within the substituted POMs are listed in Table 3. In general, most of the peak potentials are pH-dependent, indicating proton intervention in the overall redox mechanism. The other trends observed for the phosphorus analogues are also seen here. Reduction of the Cu^{2+} centre is merged with the first tungsten reduction, precluding any accurate determination of its peak potential location. Oxidation of the Mn^{2+} centre is observed, but at a highly positive potential. Oxidation of the Co^{2+} centre is difficult to achieve.

Table 3. Potential locations of the cations which may be reduced or oxidized within $\alpha_2\text{-AsW}_{17}\text{M}$ in a pH = 3.00 and a pH = 5.00 medium; E_{pc} = cathodic peak potential; E_{pa} = anodic peak potential; scan rate: 10 mVs^{-1} ; working electrode: glassy carbon; reference electrode: SCE

Reducible cations	$-E_{\text{pc}}$ [V]	
	pH = 3	pH = 5
Fe^{3+} in AsW_{17}Fe	0.150	0.230
Cu^{2+} in AsW_{17}Cu	—	0.348
Mo^{6+} in AsW_{17}Mo	−0.096	−0.082
Oxidizable cations	E_{pa} [V]	
	pH = 3	pH = 5
V^{4+} in $\text{AsW}_{17}\text{V}^{\text{IV}}$	0.456	0.378
Mn^{2+} in AsW_{17}Mn	1.060	0.892
Co^{2+} in AsW_{17}Co	—	1.406

Influence of the Central Heteroatom on the First Tungsten Reduction Wave within XW_{17}M (X = P or As)

Figure 1 (A and B) illustrate two typical examples of the limiting behaviour observed at pH = 3. For the Mn^{2+} -substituted derivatives, the peak potential for the first tungsten reduction wave is hardly displaced in Figure 1A, irrespective of whether the central heteroatom is As or P. In contrast, for the Cu^{2+} complexes, Figure 1B shows a 154 mV positive shift for the first tungsten reduction peak potential in the As compound compared with the P derivative. It must be pointed out that a combined Cu and W first wave was observed at pH = 3 for both P and As derivatives. In both cases, controlled potential coulometry beyond the peak potential of this composite wave consumes four electrons per molecule for complete reduction at pH = 3. Electrolysis conducted at the half-wave potential and combined with spectroelectrochemistry or simple inspection of the solution colour indicates that the two-electron reduction of

the Cu^{2+} centre is completed before that of the W^{6+} centres begins. The first tungsten reduction peak potentials at pH = 3 are shown in Table 4 for all the substituted derivatives along with the value for $\text{H}_4\text{AsW}_{17}$. It appears from these data that the difference $\Delta E_{\text{p}} = E_{\text{p}}(\text{lacunary}) - E_{\text{p}}(\text{substituted})$, available only for As compounds, depends on the nature of the substituent. At pH = 3, the largest effect was obtained for AsW_{17}Mo in which the first tungsten wave was driven 144 mV in the positive potential direction compared with the same wave in the lacunary precursor. All other differences are modest and range between +14 mV to −62 mV. The value of ΔE_{p} for the V^{4+} complex is remarkable and is comparable with those found for substituted derivatives bearing a terminal water molecule and not with a compound such as AsW_{17}Mo bearing a terminal oxo group. Analogous trends were also obtained previously in the study of the α_1 - and α_2 - $\text{P}_2\text{W}_{17}\text{M}$ series.^[16–18]

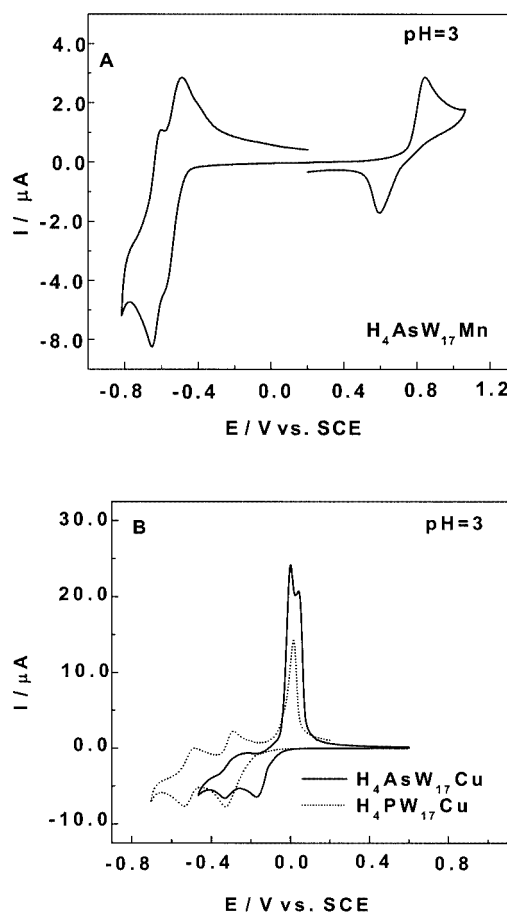


Figure 1. Cyclic voltammograms recorded on $5 \times 10^{-4} \text{ M}$ solutions of the relevant polyoxometalate in a pH = 3 medium ($0.2 \text{ M Na}_2\text{SO}_4 + \text{H}_2\text{SO}_4$); scan rate: 10 mVs^{-1} ; working electrode: glassy carbon; reference electrode: SCE; A: $\alpha\text{-}[\text{H}_4\text{Mn}(\text{H}_2\text{O})\text{AsW}_{17}\text{O}_{61}]^{9-}$; B: $\alpha\text{-}[\text{H}_4\text{Cu}(\text{H}_2\text{O})\text{AsW}_{17}\text{O}_{61}]^{9-}$ (solid line) and $\alpha\text{-}[\text{H}_4\text{Cu}(\text{H}_2\text{O})\text{PW}_{17}\text{O}_{61}]^{9-}$ (dotted line)

The influence of the nature of the central heteroatom X within XW_{17}M (X = P or As) leads to modest peak potential shifts ranging between −30 mV and +30 mV, except in the case of the Cu^{2+} -substituted derivatives. In fact, the pK_{a}

Table 4. Potential locations of the first tungsten wave for AsW₁₇M derivatives and their differences with the corresponding wave of the precursor lacunary species in a pH = 3 medium; scan rate: 10 mV·s⁻¹; working electrode: glassy carbon; reference electrode: SCE; E_{pc} : cathodic peak potential; $\Delta E_{pc} = (E_{pc \text{ lacunary}} - E_{pc \text{ substituted}})$

Substituent	$-E_{pc}$ [mV]	ΔE_{pc} [mV]
Lacunary	372	0
V ⁴⁺	400	28
Mn ²⁺	358	-14
Fe ³⁺	434	62
Co ²⁺	432	60
Ni ²⁺	420	48
Zn ²⁺	388	16
Mo ⁶⁺	280	-144

values for the substituted complexes and for their reduction species might be different, thus rendering complicated any study of the nature of the central heteroatom and of the pH effect.

Electrocatalytic Reductions of Nitrite and Nitrate

The behaviour of AsW₁₈ and its substituted derivatives AsW₁₇M towards the electrocatalytic reductions of nitrite and nitrate were tested in the pH-stable ranges of these POMs. In the potential region explored, no direct reduction of nitrite or nitrate on the glassy carbon electrode surface could be observed.^[19,20] It was also deemed interesting to look, in particular, for cases in which a catalytic current could be observed on the first wave or the first several waves of each POM, in such potential regions. Under these conditions, the processes occur in solution and, usually, no permanent modification of the electrode surface by the POM was obtained.^[21] Conclusions from our previous work^[10,12,20] were confirmed here and indicate that only Cu- and Ni-substituted derivatives catalyse the reduction of nitrate, while most derivatives catalyse the reduction of nitrite. Typically, Figure 2 (A and B) illustrates selected representative examples of electrocatalytic reductions of nitrite by AsW₁₈ or by AsW₁₇Cu, respectively. At pH = 2 and in the absence of nitrite, the first two waves of AsW₁₈ are closely spaced (Figure 2, A). Upon addition of even modest amounts of nitrite, a large cathodic current enhancement was observed (Figure 2, B). This cathodic current was slightly composite and no longer had any associated anodic counterpart. Increasing the concentration of nitrite through adjustment of the excess parameter γ ($\gamma = C_{\text{NO}_2^-}/C_{\text{POM}}$) still enhanced the cathodic current. Thus, efficient catalysis of nitrite reduction^[22] was achieved during the reduction of AsW₁₈. This current increase can be expressed more quantitatively through the catalytic efficiency CAT defined as $\text{CAT} = 100 \times [I_{(\text{POM} + \text{NO}_2^-)} - I_{\text{d}(\text{POM})}]/I_{\text{d}(\text{POM})}$ where $I_{(\text{POM} + \text{NO}_2^-)}$ represents the reduction peak current of the POM in the presence of nitrite and $I_{\text{d}(\text{POM})}$ the reduction peak current for the POM alone.

In the experiment described in Figure 2, CAT was found to vary from 634% to 1185% for $\gamma = 10$ and $\gamma = 30$, respec-

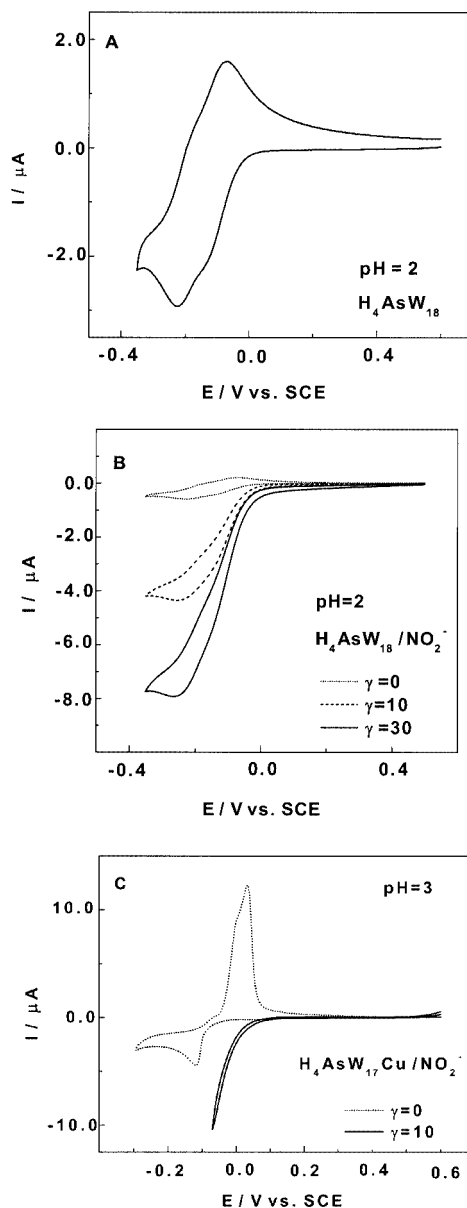


Figure 2. Cyclic voltammograms recorded on 5×10^{-4} M solutions of the relevant polyoxometalate; scan rate: 2 mV·s⁻¹; working electrode: glassy carbon; reference electrode: SCE; for the definition of the excess parameter γ , see text; A: first two waves of $\alpha\text{-[H}_4\text{AsW}_{18}\text{O}_{62}]^{7-}$ alone in a pH = 2 medium (0.2 M Na₂SO₄ + H₂SO₄); B: same conditions as in A with the addition of increasing amounts of nitrite; C: $\alpha\text{-[H}_4\text{Cu(H}_2\text{O)AsW}_{17}\text{O}_{61}]^{9-}$ in the absence and presence of nitrite in a pH = 3 medium (0.2 M Na₂SO₄ + H₂SO₄)

tively. While electrocatalysis by AsW₁₈ is triggered by reduced W centres, a more complex pathway must be considered in the case of AsW₁₇Cu. Figure 2, C shows at pH = 3 the first combined Cu/W cathodic wave for this POM with the characteristic stripping oxidation pattern on potential reversal. Superimposed on this is the cyclic voltammogram obtained in the presence of nitrite. The main obser-

variations can be summarized as follows: (i) copper deposition can be obtained upon scanning the first combined Cu/W cathodic wave; (ii) nitrite electrocatalytic reduction begins in a potential region in which the reduction current of AsW_{17}Cu is very weak; (iii) the electrocatalytic reduction of nitrite is very fast, so that no copper deposition could be detected in the potential range explored, at least as far as cyclic voltammetry is concerned.

The electrocatalytic reduction of nitrate by reduced AsW_{17}Cu adds a new example to the few described in our previous work.^[10,12,20] Figure 3 summarises the observations at pH = 3 and 5. Figure 3, A (obtained at pH = 3) shows that the nitrate electrocatalytic reduction is effective and is enhanced with increasing γ values. A comparison of Figures 2 and 3, A requires, at the very least, the following two remarks: (i) the electrocatalytic reduction of nitrite begins at a potential substantially less negative than that for the nitrate; (ii) a much larger excess parameter value is needed to observe a clear catalytic effect in the case of nitrate compared with that of nitrite. Figure 3, B indicates that the electrocatalytic reduction of nitrate remains effective at pH = 5. It is worth noting that two cathodic steps

were observed for copper reduction processes in this medium. The potential shift for nitrate reduction also falls in the range of 100 mV per pH unit. Finally, we found qualitatively that the central heteroatom X in XW_{17}Cu (X = P or As) has little influence on the electrocatalytic reduction of nitrate.

Conclusions

The present work expands our earlier results which were previously limited to the synthesis and comparison of the electrochemical behaviour of AsW_{18} and its symmetrical analogue As_2W_{18} . The monolacunary species AsW_{17} was synthesized for the first time and served as a precursor to introduce first-row transition-metal ions in the framework of the novel Dawson-type tungstomonoarsenate. Several lines of experimental evidence converge to indicate that the substitution occurs in the α_2 position. The short-term stability of AsW_{17} in solution contrasts with the instability of its phosphorus analogue. This situation allows a comparison between the electrochemical behaviour of this lacunary POM and the transition-metal ion substituted systems. Most of the latter complexes were expected to behave like the lacunary precursor, at least with respect to the redox properties of the W framework. The results confirm this expectation. The efficiency of AsW_{17}Cu towards the electrocatalytic reduction of nitrate is a new example in addition to the few previously published.

Experimental Section

Preparations: All chemicals were of reagent grade and were used as received. The isolated yields of the final pure products ranged constantly from 60 to 95% in all the preparations. $\alpha\text{-K}_7[\text{H}_4\text{AsW}_{18}\text{O}_{62}]\cdot 18\text{H}_2\text{O}$ was synthesized as described previously.^[11]

$\alpha\text{-K}_{11}[\text{H}_4\text{AsW}_{17}\text{O}_{61}]\cdot 18\text{H}_2\text{O}$ ($\text{H}_4\text{AsW}_{17}$): A sample of $\alpha\text{-K}_7[\text{H}_4\text{AsW}_{18}\text{O}_{62}]\cdot 18\text{H}_2\text{O}$ (8 g, 1.6 mmol) was dissolved in Millipore water (20 mL) with stirring. To the clear solution, was added KHCO_3 (17 mL of a 1 M solution) and a white precipitate gradually formed. Stirring was continued for roughly 1 h. The solid was then left to settle and was filtered, washed twice with ethyl alcohol, twice with diethyl ether and was air-dried by suction through a flask with an aspirator (yield 7.5 g, 95%). $\text{K}_{11}[\text{H}_4\text{AsW}_{17}\text{O}_{61}]\cdot 18\text{H}_2\text{O}$ (4934.5): calcd. As 1.52, K 8.72, W 63.34, H_2O 6.57; found As 1.59, K 8.91, W 62.81, H_2O 6.31.

$\alpha\text{-K}_9[\text{H}_4\text{Zn}(\text{H}_2\text{O})\text{AsW}_{17}\text{O}_{61}]\cdot 20\text{H}_2\text{O}$ (AsW_{17}Zn): A sample of $\text{Zn}(\text{NO}_3)_2\cdot 6\text{H}_2\text{O}$ (0.30 g, ca. 1 mmol) was dissolved in Millipore water (45 mL) and $\alpha\text{-K}_{11}[\text{H}_4\text{AsW}_{17}\text{O}_{61}]\cdot 18\text{H}_2\text{O}$ (4 g, 0.82 mmol) was added in small portions while heating the mixture on a water bath (ca. 60 °C). After 30 min, the cloudy mixture was filtered hot and the clear filtrate left in a beaker. Large white crystals appeared upon cooling. This material was filtered, washed with ethyl alcohol and left to dry in the open air (yield 2.8 g, 70%). Recrystallization was performed with a minimum amount of Millipore water. $\text{K}_9[\text{H}_4\text{Zn}(\text{H}_2\text{O})\text{AsW}_{17}\text{O}_{61}]\cdot 20\text{H}_2\text{O}$ (4975.7): calcd. As 1.51, K 7.10, W 63.07, Zn 1.32; found As 1.42, K 6.97, W 65.2, Zn 1.66.

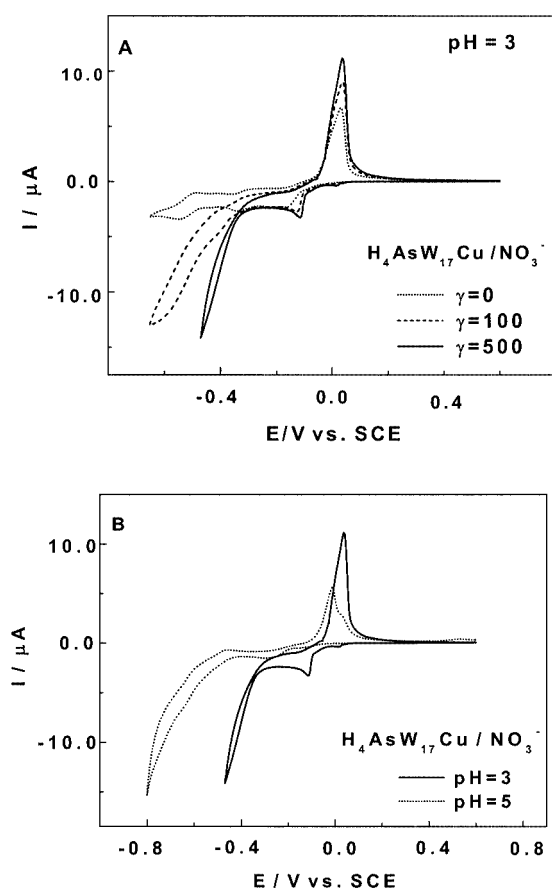


Figure 3. Cyclic voltammograms recorded on 5×10^{-4} M solutions of $\alpha\text{-}[\text{H}_4\text{Cu}(\text{H}_2\text{O})\text{AsW}_{17}\text{O}_{61}]^{9-}$ in the absence and presence of nitrate; scan rate: $2 \text{ mV}\cdot\text{s}^{-1}$; working electrode: glassy carbon; reference electrode: SCE; for the definition of the excess parameter γ , see text; A: in a pH = 3 medium ($0.2 \text{ M Na}_2\text{SO}_4 + \text{H}_2\text{SO}_4$), with increasing amounts of nitrate; B: comparison of the cyclic voltammograms run in the presence of nitrate in a pH = 3 medium and in a pH = 5 medium, respectively ($0.4 \text{ M CH}_3\text{COONa} + \text{CH}_3\text{COOH}$)

α -K₉[H₄Cu(H₂O)AsW₁₇O₆₁]·18H₂O (AsW₁₇Cu): A sample of Cu(NO₃)₂·3H₂O (0.25 g, ca. 1 mmol) was dissolved in Millipore water (45 mL) and α -K₁₁[H₄AsW₁₇O₆₁]·18H₂O (4 g, 0.82 mmol) was added in small portions while heating the mixture on a water bath (ca. 60 °C). After 30 min, the cloudy greenish mixture was filtered hot and the green clear filtrate left in a beaker. Large green crystals appeared upon cooling. This material was filtered, washed with ethyl alcohol and left to dry in the open air. Recrystallization was performed from a minimum amount of Millipore water (yield 2.6 g, 65%). K₉[H₄Cu(H₂O)AsW₁₇O₆₁]·18H₂O (4937.8): calcd. As 1.52, Cu 1.29, K 7.13, W 63.30; found As 1.60, Cu 1.27, K 7.26, W 62.81.

α -K₉[H₄Ni(H₂O)AsW₁₇O₆₁]·21H₂O (AsW₁₇Ni): A sample of Ni(NO₃)₂·6H₂O (0.30 g, ca. 1 mmol) was dissolved in Millipore water (45 mL) and α -K₁₁[H₄AsW₁₇O₆₁]·18H₂O (4 g, 0.82 mmol) was added in small portions while heating the mixture on a water bath (ca. 60 °C). After 30 min, the green clear mixture was filtered hot and the green clear filtrate left in a beaker. A pale green yellow crystalline material appeared upon cooling. This material was filtered, washed with ethyl alcohol and left to dry in the open air. Recrystallization was performed from a minimum amount of Millipore water (yield 3.8 g, 95%). K₉[H₄Ni(H₂O)AsW₁₇O₆₁]·21H₂O (4987): calcd. As 1.50, K 7.06, Ni 1.18, W 62.67; found As 1.32, K 7.03, Ni 1.24, W 63.16.

α -K₉[H₄Co(H₂O)AsW₁₇O₆₁]·18H₂O (AsW₁₇Co): A sample of Co(NO₃)₂·6H₂O (0.30 g, ca. 1 mmol) was dissolved in Millipore water (45 mL) and K₁₁[H₄AsW₁₇O₆₁]·18H₂O (4 g, 0.82 mmol) was added in small portions while heating the mixture on a water bath (ca. 60 °C). After 30 min, the dark red cloudy mixture was filtered hot and the clear dark red filtrate left in a beaker. A clear sand-coloured crystalline material appeared upon cooling. This material was filtered, washed with ethyl alcohol and left to dry in the open air. Recrystallization was performed from a minimum quantity of Millipore water (yield 3.8 g, 95%). K₉[H₄Co(H₂O)AsW₁₇O₆₁]·18H₂O (4933.2): calcd. As 1.52, Co 1.19, K 7.13, W 63.36; found As 1.46, Co 1.15, K 7.06, W 63.52.

α -K₈[H₄Fe(H₂O)AsW₁₇O₆₁]·19H₂O (AsW₁₇Fe): A sample of Fe(NO₃)₃·9H₂O (0.40 g, ca. 1 mmol) was dissolved in Millipore water (45 mL) and α -K₁₁[H₄AsW₁₇O₆₁]·18H₂O (4 g, 0.82 mmol) was added in small portions while heating the mixture on a water bath (ca. 60 °C). After 30 min, the pale yellow suspension was filtered hot and the yellow clear filtrate transferred to a beaker. Upon treatment of this filtrate with KCl (10 g), a pale yellow crystalline material appeared. This material was filtered, washed with ethyl alcohol and left to dry in the open air. Recrystallization was performed from a minimum quantity of Millipore water (yield 2.4 g, 60%). K₈[H₄Fe(H₂O)AsW₁₇O₆₁]·19H₂O (4909): calcd. As 1.53, Fe 1.14, K 6.37, W 63.67; found As 1.43, Fe 1.26, K 6.94, W 62.74.

α -K₉[H₄Mn(H₂O)AsW₁₇O₆₁]·19H₂O (AsW₁₇Mn): A sample of Mn(NO₃)₂·4H₂O (0.25 g, ca. 1 mmol) was dissolved in Millipore water (45 mL) and α -K₁₁[H₄AsW₁₇O₆₁]·18H₂O (4 g, 0.82 mmol) was added in small portions while heating the mixture on a water bath (ca. 60 °C). After 30 min, the dark beige suspension was filtered hot and the dark beige clear filtrate left in a beaker. Large chestnut-coloured crystals appeared upon cooling. This material was filtered, washed with ethyl alcohol and left to dry in the open air. Recrystallization was performed from a minimum amount of Millipore water (yield 3.6 g, 90%). K₉[H₄Mn(H₂O)AsW₁₇O₆₁]·19H₂O (4947.2): calcd. As 1.51, K 7.11, Mn 1.11, W 63.18; found As 1.47, K 7.23, Mn 1.24, W 62.40.

α -K₉[H₄AsV^{IV}W₁₇O₆₂]·18H₂O (AsW₁₇V^{IV}): A sample of VOSO₄·5H₂O (0.42 g, 1.7 mmol) was dissolved in Millipore water (90 mL) and acidified with 4 M HCl (8.5 mL). α -K₁₁[H₄AsW₁₇O₆₁]·18H₂O (8 g, 1.64 mmol) was then added in small portions with stirring. The black solution was stirred for roughly 30 min and then filtered and treated with KCl (10 g). The grey black precipitate that resulted was filtered, washed with ethyl alcohol and dried in the open air. This material was recrystallized from a minimum of acidified water (HCl solution pH < 1) (yield 5.6 g, 70%). K₉[H₄AsV⁽⁴⁺⁾W₁₇O₆₂]·18H₂O (4923.2): calcd. As 1.52, K 7.15, V 1.03, W 63.48; found As 1.55, K 8.14, V 0.99, W 64.7.

α -K₈[H₄AsV^VW₁₇O₆₂]·18H₂O (AsW₁₇V^V): A sample of NaVO₃ (0.21 g, 1.7 mmol) was dissolved in Millipore water (90 mL) and acidified with 4 M HCl (8.5 mL). α -K₁₁[H₄AsW₁₇O₆₁]·18H₂O (8 g, 1.64 mmol) was then added in small portions with stirring. The yellow solution was stirred for roughly 30 min, filtered, then treated with KCl (10 g). The yellow precipitate that resulted was filtered, washed with ethyl alcohol and dried in the open air. This material was recrystallized from a minimum of acidified water (HCl solution pH < 1) (yield 4.8 g, 60%). K₈[H₄PV⁽⁵⁺⁾W₁₇O₆₂]·18H₂O (4884.1): calcd. As 1.53, K 6.40, V 1.04, W 63.99; found As 1.61, K 6.27, V 1.00, W 63.2.

α -K₇[H₄AsMoW₁₇O₆₂]·18H₂O (AsW₁₇Mo): A sample of Na₂MoO₄·2H₂O (0.40 g, 1.7 mmol) was dissolved in Millipore water (90 mL) and acidified with 4 M HCl (8.5 mL). α -K₁₁[H₄AsW₁₇O₆₁]·18H₂O (8 g, 1.64 mmol) was then added in small portions whilst stirring. The clear yellow solution was stirred for roughly 30 min, then filtered and treated with KCl (10 g). The fine yellow precipitate that resulted was filtered, washed with ethyl alcohol and dried in the open air. This material was recrystallized from a minimum of acidified water (HCl solution pH < 1) (yield 4.4 g, 55%). K₇[H₄AsMoW₁₇O₆₂]·18H₂O (4890): calcd., As 1.53, K 5.60, Mo 1.96, W 63.92; found As 1.49, K 5.33, Mo 1.61, W 65.27.

General Methods and Materials: Pure water was used throughout. It was obtained by passing through a RiOs 8 unit followed by a Millipore-Q Academic purification set. All reagents were of high-purity grade and were used as purchased without further purification. Elemental analyses were performed by Kanti Labs Ltd, Mississauga, Canada. The IR spectra were recorded in KBr pellets with a Perkin-Elmer Spectrum One FT-IR spectrophotometer. The UV/Vis spectra were recorded with a Perkin-Elmer Lambda 19 spectrophotometer on 2.5×10^{-5} M solutions of the relevant polyanion. Matched 1.000-cm optical path quartz cuvettes were used. The compositions of the various media were as follows: for pH = 0.33: 0.5 M H₂SO₄; for pH = 1–3: 0.2 M Na₂SO₄ + H₂SO₄; for pH = 4 and 5: 0.4 M CH₃COONa + CH₃COOH; for pH = 6 and 7: 0.4 M NaH₂PO₄ + NaOH.

Electrochemical Experiments: The media used for UV/Vis spectroscopy were also used for electrochemistry except that the polyanion concentration was 5×10^{-4} M. All cyclic voltammograms were recorded at a scan rate of 10 mV·s⁻¹ unless otherwise stated. The solutions were deoxygenated thoroughly for at least 30 min with pure argon and kept under a positive pressure of this gas during the experiments. The source, mounting and polishing of the glassy carbon (GC, Tokai, Japan) electrodes has been described.^[23] The glassy carbon samples had a diameter of 3 mm. The electrochemical apparatus was an EG & G 273 A driven by a PC with the M270 software. Potentials are quoted relative to the saturated calomel electrode (SCE). The counter electrode was a platinum gauze of large surface area. All experiments were performed at room temperature.

Acknowledgments

This work was supported by the CNRS (UMR, 8000 and UMR 7071), the Universities Paris XI, Paris VI and Georgetown University. We also thank Benoît Faure for assistance with several electrochemistry experiments.

- [1] M. T. Pope *Heteropoly and Isopoly Oxometalates*, Springer-Verlag, Berlin, **1983**.
- [2] M. T. Pope; A. Müller, *Angew. Chem. Int. Ed. Engl.* **1991**, *30*, 34–48.
- [3] *Polyoxometalates: From Platonic Solids to Anti-Retroviral Activity* (Eds.: M. T. Pope, A. Müller), Kluwer, Dordrecht, The Netherlands, **1994**.
- [4] Topical issue on polyoxometalates: C. L. Hill, *Chem. Rev.* **1998**, *98*, 1–389.
- [5] *Polyoxometalate Chemistry: From Topology via Self-Assembly to Applications* (Eds.: M. T. Pope, A. Müller), Kluwer, Dordrecht, The Netherlands, **2001**.
- [6] *Polyoxometalate Chemistry for Nano-Composite Design* (Eds.: T. Yamase, M. T. Pope), Nanostructure Science and Technology, Kluwer Academic/Plenum Publishing, New York, **2002**.
- [7] M. T. Pope, *Polyoxo Anions: Synthesis and Structure in Comprehensive Coordination Chemistry II*, vol. 4 (Ed.: A. G. Wedd), Elsevier Science, New York **2004**, p. 635–678.
- [8] C. L. Hill, *Polyoxometalates: Reactivity in Comprehensive Coordination Chemistry II*, vol. 4 (Ed.: A. G. Wedd), Elsevier Science, New York **2004**, p. 679–759.
- [9] R. Contant, S. Piro-Sellem, J. Canny, R. Thouvenot, *C. R. Acad. Sci., Ser. IIC:Chim.* **2000**, *3*, 157–161.
- [10] B. Keita, I. M. Mbomekalle, L. Nadjo, R. Contant, *Electrochem. Commun.* **2001**, *3*, 267–273.
- [11] I. M. Mbomekalle, B. Keita, L. Nadjo, R. Contant, N. Belai, M. T. Pope, *Inorg. Chim. Acta* **2003**, *342*, 219–228.
- [12] I. M. Mbomekalle, B. Keita, L. Lu, L. Nadjo, R. Contant, N. Belai, M. T. Pope, *Eur. J. Inorg. Chem.* **2004**, 276–285.
- [13] R. Contant, M. Abbessi, J. Canny, A. Belhouari, B. Keita, L. Nadjo, *Inorg. Chem.* **1997**, *36*, 4961–4967.
- [14] T. L. Jorjris, M. Kozik, N. Casan-Pastor, P. J. Domaille, R. G. Finke, W. K. Miller, L. C. W. Baker, *J. Am. Chem. Soc.* **1987**, *109*, 7402–7408.
- [15] B. Keita, A. Belhouari, L. Nadjo, R. Contant, *J. Electroanal. Chem.* **1998**, *442*, 49–57.
- [16] B. Keita, Y. W. Lu, L. Nadjo, R. Contant, M. Abbessi, J. Canny, M. Richet, *J. Electroanal. Chem.* **1999**, *477*, 146–157.
- [17] B. Keita, F. Girard, L. Nadjo, R. Contant, J. Canny, M. Richet, *J. Electroanal. Chem.* **1999**, *478*, 76–82.
- [18] R. Contant, M. Abbessi, J. Canny, M. Richet, B. Keita, A. Belhouari, L. Nadjo, *Eur. J. Inorg. Chem.* **2000**, 567–574.
- [19] A. Belhouari, B. Keita, L. Nadjo, R. Contant, *New J. Chem.* **1998**, 83–86.
- [20] B. Keita, E. Abdeljalil, L. Nadjo, R. Contant, R. Belghiche, *Electrochem. Commun.* **2001**, *3*, 56–62.
- [21] B. Keita, L. Nadjo, *Mater. Chem. Phys.* **1989**, *22*, 77–103.
- [22] At pH = 1, the actual active species should be HNO_2 and/or NO. In fact, the following sequence is known: $\text{HNO}_2 \rightarrow \text{H}^+ + \text{NO}_2^-$ $\text{p}K_{\text{a}} = 3.3$ at 18 °C and HNO_2 disproportionates in fairly acidic solution: $3 \text{HNO}_2 \rightarrow \text{HNO}_3 + 2 \text{NO} + \text{H}_2\text{O}$. The rate of this reaction is known to be low.
- [23] B. Keita, F. Girard, L. Nadjo, R. Contant, R. Belghiche, M. Abbessi, *J. Electroanal. Chem.* **2001**, *508*, 70–80.

Received March 8, 2004

Early View Article

Published Online August 12, 2004